JOURNAL OF MATERIALS SCIENCE 23 (1988) 4450–4462

Some elevated temperature mechanical properties of Magnox AL80

Y. P. LIN*
H. H. Wills Physics Laboratory, University of Bristol, Tyndall Avenue, Bristol BS8 1TL, UK
G. C. SMITH
Department of Materials Science and Metallurgy, University of Cambridge, Pembroke Street, Cambridge CB2 3QZ, UK

The influence of grain-boundary hydride (MgH_2) precipitation on the mechanical properties of Magnox AL80 has been investigated by carrying out slow tensile and fatigue tests. The presence of hydride precipitates at some grain boundaries was found to have a detrimental effect on the slow tensile ductilities at the lower end (20 to 40% h^{-1}) of the range of strain rates used (20 to 2000% h^{-1}) at 250° C and at 20% h^{-1} at 300° C. Grain-boundary cavities caused by the dissociation of the hydride precipitates were introduced either by *in situ* thermal treatment prior to testing at 250° C or by testing at higher temperatures and also resulted in lower tensile ductilities at slow strain rates. The fatigue lives of Magnox AL80 were not significantly influenced by the presence of grain-boundary hydride precipitates or cavities due to the dissociation of the precipitates. This is due to the majority of the boundaries being unsuitably oriented to experience high shear stresses. Long-term ageing at 450° C was found to reduce the subsequent fatigue strength at that temperature and this effect is associated with the boundaries becoming more prone to migration during fatigue cycling.

1. Introduction

In a previous paper [1], a grain-boundary precipitation phenomenon in Magnox AL80 was investigated and the precipitate confirmed as magnesium hydride, MgH_2. Because Magnox AL80 was developed mainly for elevated temperature use, it is pertinent to consider the influence of hydride precipitates on the elevated temperature mechanical properties. The creep properties of Magnox AL80 as a function of stress, temperature and grain size have been summarized previously [2] and the creep behaviour has been interpreted [3] in terms of the interaction of dislocations (in the basal planes) with solute (Al) atoms and the cross-slip of dislocations from basal to prismatic planes. Earlier work [4] had shown that at a given temperature, the highest tensile ductilities are obtained at moderate rates of strain, and that the ductility decreases with increasing time to rupture, i.e. at creep rates of strain, and also with increasing grain size. Furthermore, a ductility trough in the temperature range of approximately 200 to 300° C at low rates of strain, particularly for coarse-grained material, was found to be associated with grain-boundary cavitation, even though the maximum extent of cavitation did not coincide with the temperature of lowest ductility. The nucleation of cavities on sliding boundaries has been suggested to be possible at ledges [5], intersections with subgrains [6, 7] and at second-phase particles [8]. Subsequent cavity growth has been attributed to vacancy condensation [9], with the process controlled by dislocation movements in the grain interior [10], although an alternative mechanism involving the annihilation of the dislocations which are responsible for the boundary sliding has also been proposed [11].

The fatigue properties of Magnox AL80 are influenced by grain size, test temperature, stress level and frequency [4, 12], such that high stresses and low test frequencies above 225° C favour failure by intergranular cracking, while low stresses and high frequencies favour grain-boundary cavitation. The fatigue strength decreases with decreasing grain size and with increasing temperature, but remains approximately constant, or even shows a slight increase, for long-term tests between 400 and 500° C. Grain-boundary cavitation is associated with grain-boundary migration to positions at 45° to the stress axis [13, 14], which suggests that extensive cavity nucleation and growth takes place after the 45° structure is attained [14], particularly as grain growth and boundary migration have been shown to be affected by the presence of cavities [15].

Grain-boundary cracking and cavitation can be influenced by the presence of grain-boundary precipitates, which suggests that the grain-boundary hydride precipitates, and their dissociation behaviour, reported previously [1], may affect the elevated temperature mechanical properties of Magnox AL80. This has been investigated in the present work by the determination of slow tensile and fatigue properties on material subjected to different heat treatments.

* *Present address*: Department of Materials Science and Engineering, McMaster University, 1280 Main Street West, Hamilton, Ontario, Canada L8S 4L7

0022–2461/88 $03.00 + .12

TABLE I Manufacturer's chemical analysis (wt %)

Cast number	Al	Si	Mn	Fe	Ca	Zn	Be	H (p.p.m.)	Mg
B	0.82	0.005	0.006	0.005	< 0.005	0.007	0.005	11	Balance
C	0.84	0.005	0.007	0.005	< 0.005	0.002	0.004	9	Balance
D	0.84	0.008	0.005	0.003	< 0.005	0.004	0.005	12	Balance

2. Materials and experimental details

Three batches (B, C and D) of Magnox AL80 were used and the analyses are given in Table I. For tensile tests, an Instron testing machine with variable cross-head speeds was used, with specimens of 4.5 mm gauge diameter and 15 mm gauge length. Constant cross-head speeds were used so that all strain rates quoted are the initial values.

Fatigue tests were carried out at room temperature (RT) using an Amsler Vibrophore in push-pull (stress ratio $R = -1$) at 150 Hz and at elevated temperatures using a Schenck Midget Pulsator in push-pull at 50 Hz. Hour-glass fatigue test specimens of 25 mm gauge length but different gauge diameters were used for tests at different temperatures (15 mm for 450° C, 12 mm for 350° C and 10 mm for 250° C and RT).

For elevated temperature tensile and fatigue tests, the specimens and grips were enclosed in an electric resistance furnace and each specimen was held for 1 h at the test temperature prior to testing. After specimen heat treatment, the surface oxide layer was removed by abrading with SiC paper, followed by chemical polishing in a solution of 10% HNO_3 in H_2O which also revealed the grain structure. Surface grain size was then determined using a linear intercept method, and finally, the gauge section was hand polished with Brasso metal polish.

The solvus temperature for the hydride precipitates was shown in the previous investigation to be approximately 320° C for the hydrogen contents of the batches of Magnox used. Hence to generate different precipitate distributions prior to testing, specimens were given one of the following heat treatments.

(i) Furnace-cool (FC) to RT after 2 h at 580° C. Large and few in number grain-boundary hydride precipitates.

(ii) Water-quench (WQ) to RT after 2 h at 580° C. Very fine grain-boundary hydride precipitates on some grain boundaries.

(iii) WQ treatment then aging (WQ + Age) at 250° C for 24 h and water-quench to RT. Arrays of coarser grain-boundary hydride precipitates on some grain boundaries.

For fatigue tests at 450° C, some samples were given the WQ treatment and aged at 450° C for up to 2000 h.

TABLE II Results of slow tensile tests at room temperature and at an initial strain rate of 20% h^{-1} (Batch C)

Heat treatment	Elongation (%)	0.2% proof stress, PS ($MN m^{-2}$)	UTS ($MN m^{-2}$)	PS/UTS (%)
FC	13	64	152	42
WQ	11	90	155	58
WQ + Age	12	80	144	56

3. Slow tensile properties

3.1. Influence of hydride precipitates at RT and 250° C

The tensile properties for batch C at RT and an initial strain rate of 20% h^{-1} are given in Table II. The main difference between the heat treatments is the lower normalized proof stress (PS/UTS) for the FC condition. FC specimens showed transgranular fracture, Fig. 1, while the WQ and WQ + Age fractures, although mainly transgranular, also showed occasional intergranular regions. In the WQ specimen, precipitates could not be resolved on the intergranular facets, Fig. 2, although the presence of small dimples suggests fracture by microvoid coalescence associated with fine precipitates. The WQ + Age specimen showed more intergranular regions than the WQ specimen, and these showed hydride precipitates, Fig. 3, some of which were cracked.

The tensile properties at 250° C and a strain rate of 20% h^{-1} for batch D are given in Table III. As with batch C at RT, the FC specimens showed a lower normalized proof stress than the WQ and WQ + Age specimens. The FC specimens also showed a higher elongation to failure mainly as a result of greater reduction in cross-section at fracture. It should be noted that with the WQ specimens some hydride precipitation and growth will have occurred at 250° C, during the 1 h hold prior to testing.

The WQ and WQ + Age specimens fractured by ductile intergranular mechanisms with dimples on boundary facets, Fig. 4a. However, the dimples, Fig. 4b, were not well defined and the numerous fine features preclude the clear detection of any precipitates. In contrast, the FC specimens showed coarser dimples, Fig. 5, and the greater reduction in cross-sectional area indicated that the final fracture path was unlikely to have been intergranular.

Examination of longitudinal sections of fractured specimens showed that the lower elongations of the

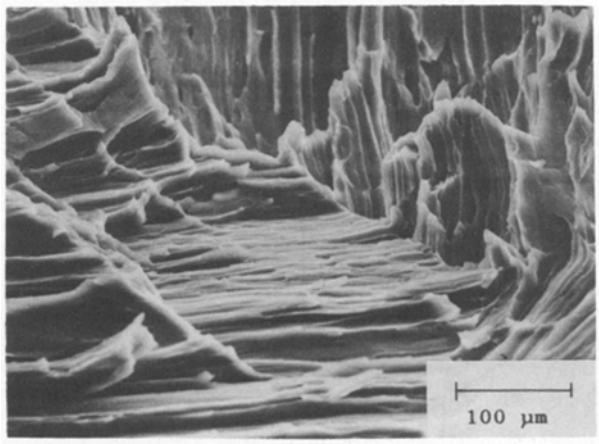

Figure 1 Fracture surface of an FC specimen fractured at RT.

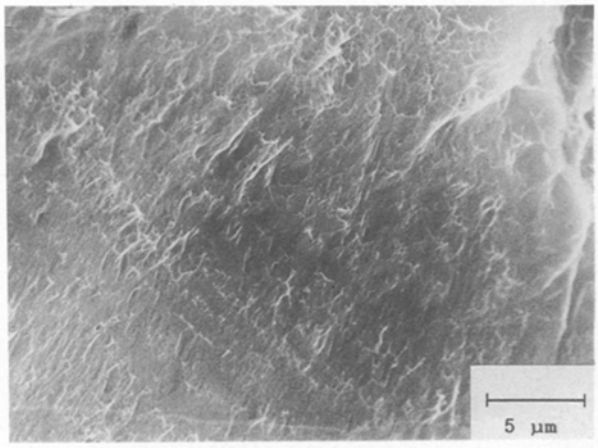

Figure 2 Grain-boundary facet on fracture surface of a WQ specimen fractured at RT.

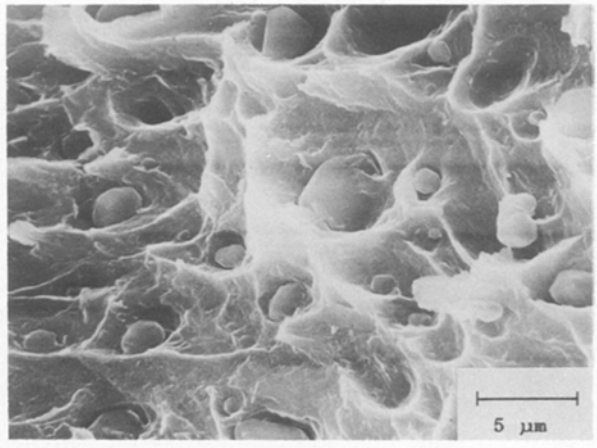

Figure 3 Grain-boundary facet on fracture surface of a WQ + Age specimen fractured at RT.

WQ and WQ + Age specimens were associated with intergranular cracks and cavities. By sectioning samples strained to different extents, grain-boundary cracks and cavities in the WQ and WQ + Age specimens were detected soon after the ultimate tensile strength, (UTS) Fig. 6, whereas no such effects were present in FC specimens strained to similar elongations. However, with FC specimens, offsets between surface grains were observed, Fig. 7, suggesting that some grain-boundary sliding had occurred.

The variation of elongation to failure with strain rate at 250° C for batch C is shown in Fig. 8. At high strain rates (above 200% h^{-1}) the values for all three heat treatments were similar but at lower strain rates the WQ and WQ + Age specimens showed lower elongations than the FC, due to greater tendency for grain-boundary failure.

The grain-boundary cracks and cavities in the WQ and WQ + Age specimens tested at 20% h^{-1}, Figs 4b and 6, were not identified unambiguously to be associated with grain boundaries containing the hydride precipitates. However, examination of the fracture surface of a WQ + Age sample tested at 800% h^{-1} revealed the presence on some boundary surfaces, Fig. 9, of cracked precipitates. It is possible that at slower strain rates, the precipitates were cracked and broken up by shearing of the sliding boundaries, so that the resulting fragments were indistinguishable from the matrix features, Fig. 4b. The tensile results suggest, however, that arrays of hydride precipitates on some boundaries in the WQ and WQ + Age specimens, reduced the overall ductility by initiating cavities. Larger grain-boundary hydride precipitates were present in the FC specimens, but the small number of such precipitates reduced their effect on ductility.

3.2. Influence of cavities at 250° C

It has been shown previously [1] that when the hydride precipitates are reheated above the solvus (~ 320° C) they will dissolve in the matrix, but simultaneously dissociate to produce cavities. The influence of this on the tensile properties was investigated by carrying out one of two *in situ* thermal treatments prior to testing at 250° C. In the first (A), specimens (FC, WQ and WQ + Age) were heated up to 450° C, held for 0.5 h and cooled over 15 min to 250° C (fast cool) held for 2 h prior to testing at a strain rate of 20% h^{-1}. The second treatment (B) was similar except the cooling from 450 to 250° C was over 110 min (slow cool). With both treatments the initial heating to 450° C would result in dissolution of the hydride and also the formation of some grain-boundary cavities due to the simultaneous dissociation of the hydride. These cavities would be relatively few in number with the FC condition due to the coarse spacing of the initial hydride precipitates and such cavities would be expected to have only a small deleterious effect on the ductility. However, the finer spacing of precipitates in the WQ + Age condition would lead to more grain-boundary cavities, and a potentially greater reduction in ductility [16, 17]. Subsequently, with treatment A, the fast cool through the solvus and hold at 250° C would enable fine hydride precipitates to form at a number of grain boundaries, thus generating a structure similar to the original WQ + Age, and having a similar ductility. The slower cool to 250° C used in treatment B would produce a few large and isolated precipitates which would have relatively little detrimental influence on ductility, i.e. a structure and properties similar to the original FC condition. Tables IV and V summarize the results, and the elongations

TABLE III Results of slow tensile tests at 250° C and at an initial strain rate of 20% h^{-1} (Batch D)

Heat treatment	Elongation (%)	0.2% proof stress, PS ($MN m^{-2}$)	UTS ($MN m^{-2}$)	PS/UTS (%)	True uniform strain (%)
FC	55.7	22.3	36.7	61	12.5
FC	48.0	22.1	37.4	59	12.1
WQ	32.3	26.7	37.8	71	9.4
WQ	32.3	25.9	38.3	68	9.8
WQ + Age	32.3	25.6	37.6	68	10.9
WQ + Age	32.3	26.2	37.7	69	9.7

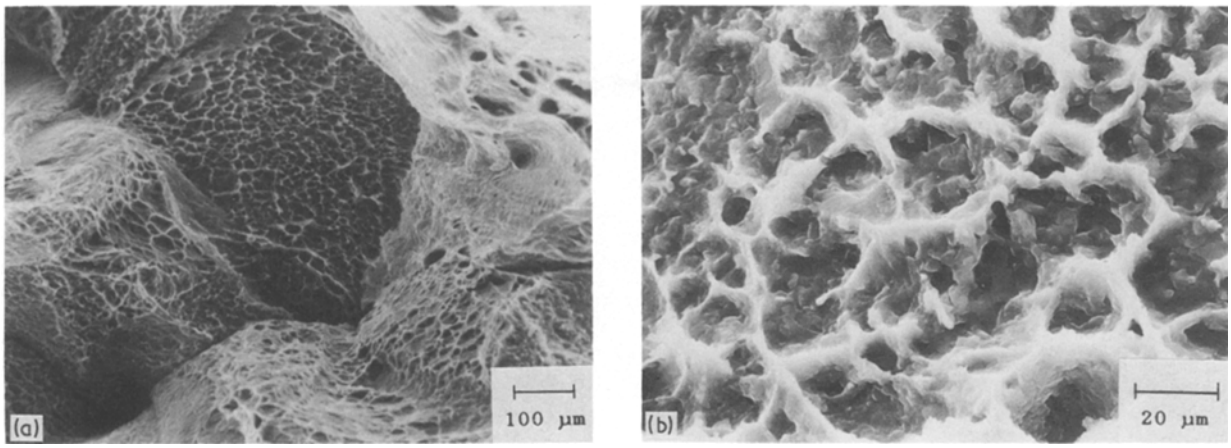

Figure 4 (a) Fracture surface of a WQ + Age specimen strained at 20% h^{-1} at 250° C. (b) Features on boundary facet in the above specimen.

to failure are also shown in Fig. 10 together with those of samples tested in the original heat-treated conditions. For the FC specimens, the high initial elongation was reduced by the fast cool from 450 to 250° C, while a slow cool had no adverse effect. For the WQ specimens, the lower elongation in the as-treated condition was increased slightly by the fast cool, and the slow cool produced a greater improvement. With the WQ + Age specimens, the elongation was improved a little by the fast cool but not by the slow cool.

On sectioned surfaces of fractured samples, the reduced ductility of the FC condition after treatment A was found to be associated with the presence of grain-boundary cracks and cavities. Conversely, the increased ductility of the WQ material with the slow cool condition was associated with very few grain-boundary cracks and cavities. Examination of the fracture surfaces of WQ + Age test samples with prior heating to 450° C showed the presence of fine particles (previously identified as probably Mg_2Si [1]) inside cavities on some boundary surfaces, Fig. 11. Such fine particles were typically associated with cavities produced by the dissociation of hydride precipitates when they were reheated to higher temperatures [1]. The form of the cavities and fine particles produced in this way and shown in Fig. 11 is clearly different from the cavities shown in Figs 4a and b, which are also from a WQ + Age specimen but tested in the as-treated condition.

TABLE IV Results of slow tensile tests at 250° C and at an initial strain rate of 20% h^{-1} after a prior *in situ* fast cool from 450 to 250° C (Batch C)

Initial heat treatment	Elongation (%)	Proof stress, PS ($MN\,m^{-2}$)	PS/UTS (%)	True uniform strain (%)
FC	44.5	19.1	59	10.4
FC	50.0	22.2	64	12.4
FC	53.7	20.9	63	10.6
WQ	44.2	23.3	62	11.0
WQ	40.1	21.2	62	12.2
WQ + Age	42.7	23.9	70	8.9
WQ + Age	43.3	24.0	70	9.2

TABLE V Results of slow tensile tests at 250° C and at an initial strain rate of 20% h^{-1} after a prior *in situ* slow cool from 450 to 250° C (Batch C)

Initial heat treatment	Elongation (%)	Proof stress, PS ($MN\,m^{-2}$)	PS/UTS (%)	True uniform strain (%)
FC	61.0	22.1	60	9.8
WQ	54.3	20.6	63	10.3
WQ	53.0	19.6	63	10.4
WQ + Age	39.8	21.5	64	9.1
WQ + Age	35.4	20.5	63	8.3

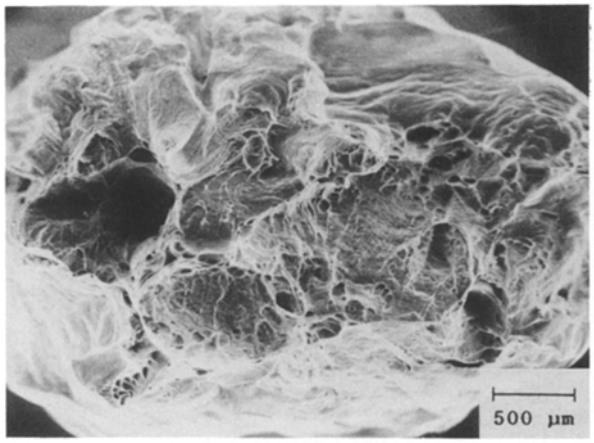

Figure 5 Fracture surface of an FC specimen strained at 20% h^{-1} at 250° C.

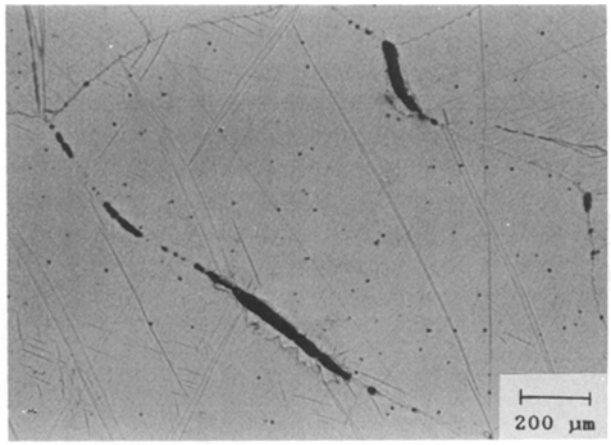

Figure 6 Sectioned surface of a WQ specimen strained at 20% h^{-1} at 250° C to just past the UTS.

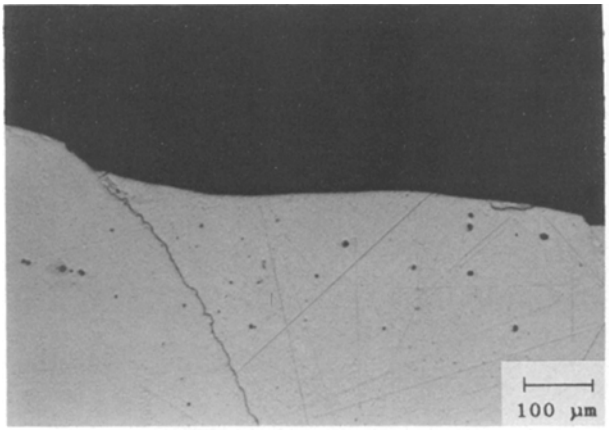

Figure 7 As Fig. 6 but for an FC specimen.

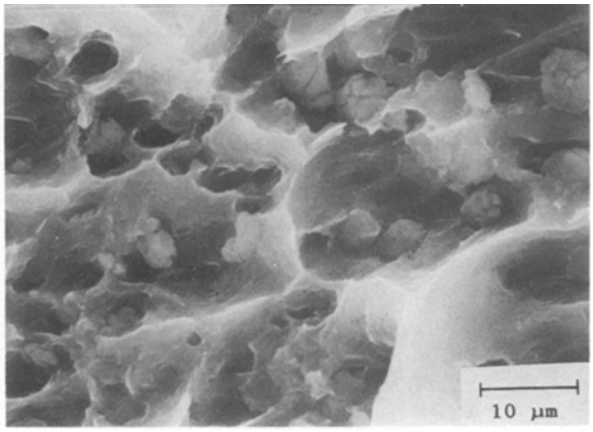

Figure 9 Grain-boundary hydride precipitates on fracture surface of a WQ + Age specimen strained at 800% h^{-1} at 250° C.

3.3. Influence of test temperature

The variation of the elongation to failure at a strain rate of 20% h^{-1} with the test temperature ranging from 250 to 450° C for specimens from batch C is shown in Fig. 12. At 350° C and above, i.e. above the hydride precipitate solvus temperature of ~ 320° C, all samples failed by extensive necking down to almost a point and the elongations to failure fell within a scatter band but with the WQ + Age specimens forming the lower limits of the scatter band at 350 and 400° C. The lower ductilities of the WQ + Age specimens at 350 and 400° C is again consistent with the dissociation of the hydride precipitates to form cavities during the 1 h pre-heating at the test temperature. At 250 and 300° C, the WQ and WQ + Age specimens, both of which would have arrays of hydride precipitates on some boundary facets, behaved similarly with lower elongations and small degrees of necking, while the FC specimens showed higher elongations and higher reductions in area. It is worthy of note that the temperature range 250 to 300° C over which differences in ductilities existed between the FC and other specimens, is not only below the hydride solvus temperature, but is also the temperature range over which Magnox AL80 exhibits a ductility trough [4]. It is possible that grain-boundary hydride precipitation may contribute to the ductility trough phenomenon but it cannot be the main cause. This follows because the FC specimens, which contained a few large hydride precipitates, which would not have a pronounced influence on the overall ductilities, also showed lower elongations at 250 and 300° C than at higher temperatures. The reduction in elongations in the WQ and WQ + Age samples due to the presence of arrays of grain-boundary hydride precipitates is thus superimposed on the ductility trough phenomenon.

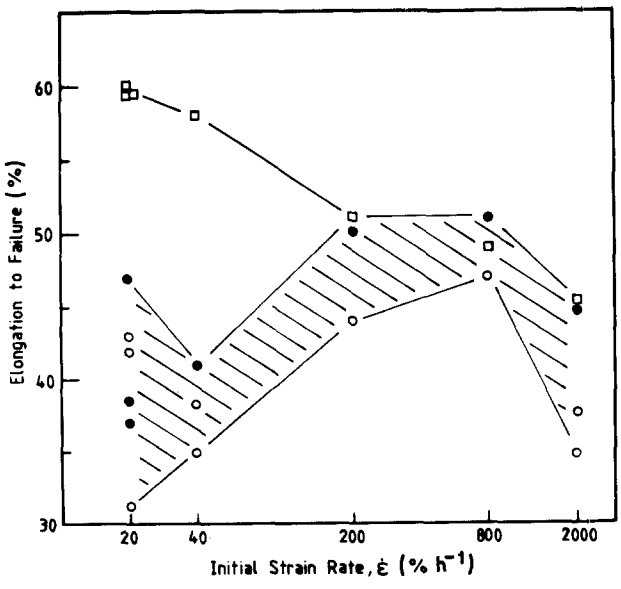

Figure 8 Variation of elongations to failure with initial strain rate at 250° C. (□) FC, (○) WQ, (●) WQ + Age.

4. Fatigue properties

4.1. Influence of hydride precipitation

The S–N_f curves for fatigue tests at room temperature are shown in Fig. 13. The fatigue lives at a given stress decrease in the order of WQ, FC and WQ + Age specimens. However, the differences are small and the superior fatigue lives of the WQ specimens, particularly

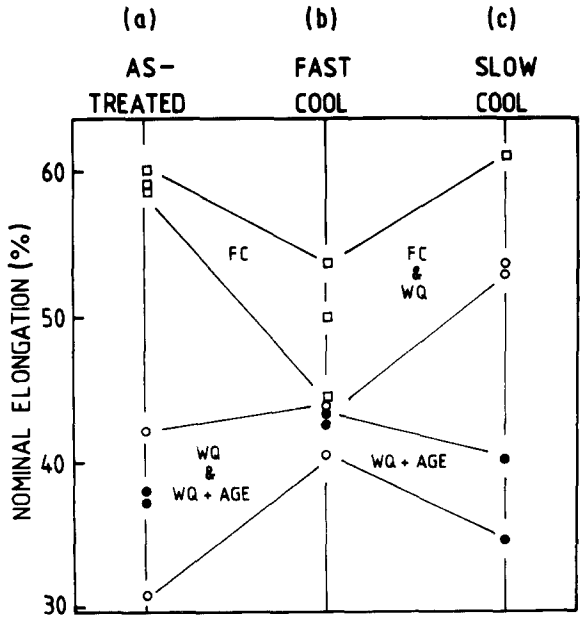

Figure 10 Variation of elongations to failure for samples tested at 250° C (a) in the as-treated condition; (b) with a prior *in situ* fast cool from 450 to 250° C, and (c) with a prior *in situ* slow cool from 450 to 250° C. (□) FC, (○) WQ, (●) WQ + Age.

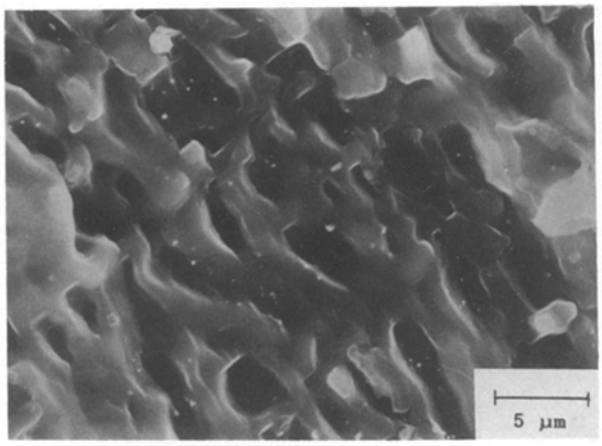

Figure 11 Grain-boundary facet on fracture surface of a WQ + Age specimen fractured at 250° C after a prior *in situ* slow cool from 450 to 250° C.

in comparison with the WQ + Age specimens, may have been due to the surface compressive stresses introduced by the water quench, which also caused twinning of the surface grains, Fig. 14. The twinning of the surface grains was not removed by the ageing treatment in the WQ + Age specimens, but residual stresses would be reduced. Failures in all cases were transgranular which indicated that the hydride precipitation at grain boundaries had negligible influence on behaviour.

The S–N_f curves for tests at 250 and 350° C are shown in Figs 15 and 16. At 250° C there is a change-over in order of fatigue lives at approximately $\pm 19\,MN\,m^{-2}$ which is associated with the transition from intergranular failures at low stresses to transgranular failures at high stresses. This was true of samples in all three heat-treated conditions and is illustrated by Fig. 17, which is for an FC specimen tested at a low stress level of $\pm 16\,MN\,m^{-2}$, and Fig. 18, which is for a WQ + Age specimen tested at a high stress level of $\pm 22\,MN\,m^{-2}$. These observations are in accord with previous results [4] which showed that transition from transgranular failures at low temperatures to intergranular failures at high temperatures was stress dependent.

At low stresses at 250° C and most stresses at 350° C, the fatigue strength decreases in the order WQ, WQ + Age and FC. There is also an indication of a cross-over in the curves at 350° C at shorter lives. At 450° C, the majority of the specimens tested were in the FC or the WQ condition. Samples from all three batches were tested and results are shown, Fig. 19. It is apparent that the data points are better grouped by their heat treatments than by batch. Examination of the tested samples showed that the twinning of surface grains in the as-treated WQ specimens was removed during the testing at 450° C. Fractures were intergranular and the fracture surfaces showed that copious cavitation had taken place at the grain boundaries, Fig. 20. Because, independent of the original treatment, all specimens would be single phase at 450° C, the superior fatigue strength of the WQ specimens compared with the FC specimens, was probably associated with the recrystallization of the surface grains. This would delay the onset of grain-boundary sliding and hence also general grain-boundary cavitation.

In addition to the FC and WQ specimens, a few samples which had been aged at 250° C for 16 days following a WQ treatment were also tested at 450° C. In these samples, cavities would be present on some boundaries after the 1 h preheating at 450° C. The fatigue lives were similar to those of the WQ specimens indicating that the presence of pre-existing cavities on some boundaries did not have any detrimental effects under conditions where rapid cavitation could take place during the fatigue tests.

For a pre-existing cavity to act as an effective cavity nucleus it must be thermodynamically stable, and the critical cavity radius, r_{crit}, is given by [18, 19]

$$r_{crit} > 4\gamma kT/\sigma^2\Omega$$

where γ is the surface energy of the matrix, k the Boltzmann constant, T the temperature, σ the applied stress across the boundary and Ω the atomic volume. For boundaries experiencing the maximum shear stresses, i.e. at 45° C to the stress axis, the shear and normal stresses are both $\sigma_0/2$ where σ_0 is the applied stress amplitude. Using $\gamma = 0.6\,J\,m^{-2}$ and $\Omega = 2.7 \times 10^{-29}\,m^3$ the critical radius, r_{crit}, would be 395 μm for

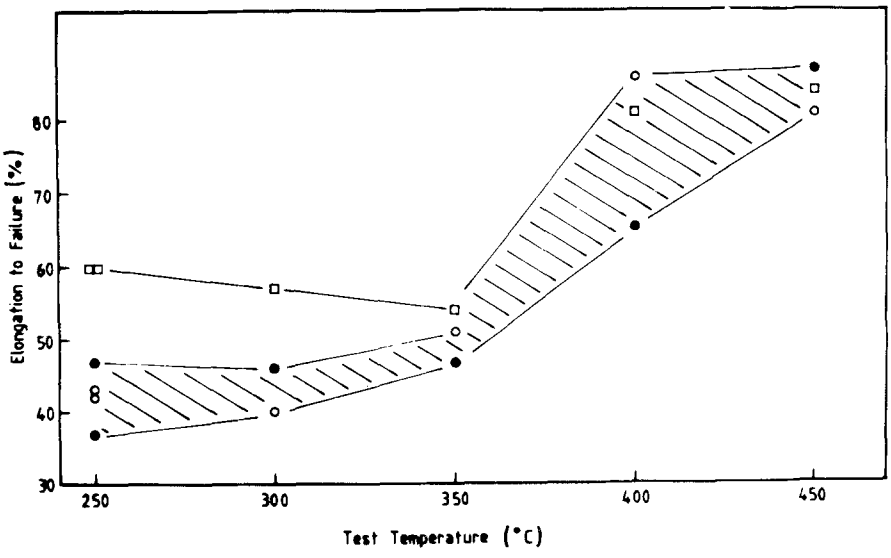

Figure 12 Variation of elongations to failure with test temperature for an initial strain rate of 20% h^{-1}. (□) FC, (○) WQ, (●) WQ + Age.

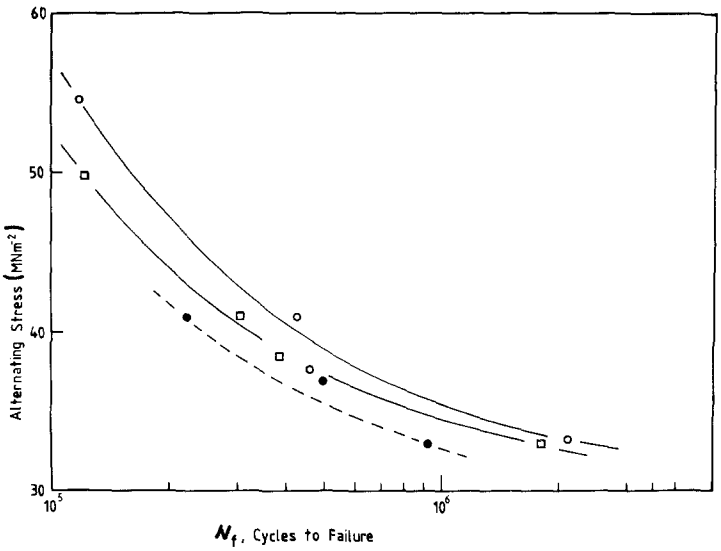

Figure 13 S–N_f curves for fatigue tests at RT. (□) FC. (○) WQ, (●) WQ + Age.

$\sigma_0 = 3\,\mathrm{MN\,m^{-2}}$ at 450° C and 48 μm for $\sigma_0 = 8\,\mathrm{MN\,m^{-2}}$ at 350°C, i.e. much larger than the typical sizes of the pre-existing cavities of not more than a few micrometres. However, r_{crit} can be greatly reduced if the sliding boundary is non-planar [19, 20]. For a boundary with sinusoidal form of wavelength λ and amplitude h, the local normal stress across the boundary is increased by a factor of $2\lambda/\pi h$ with consequent reduction in r_{crit} [20]. Using a value of 0.01 for h/λ [19], r_{crit} for the above stress levels and temperatures becomes, respectively, 0.1 μm at 450° C and 0.01 μm 350° C. Thus micrometre-sized pre-existing cavities can act as effective cavity nuclei with the aid of the stress concentration effect. However, for the stress concentration effect to be generated at boundary irregularities, of which grain-boundary cavities may be a type, grain-boundary sliding is a prerequisite. Because grain-boundary sliding is favoured for boundaries which experience high shear stresses, i.e. at or near to 45° to the stress axis, it would be expected that little or no stress concentration effects would be experienced by pre-existing cavities on boundaries located away from positions at 45° to the stress axis. Because in the present experiments the pre-existing cavities were due to the dissociation at 350 or 450° C of the hydride precipitates formed during ageing at 250° C and as not all grain boundaries exhibited the precipitation phenomenon, only a small fraction of the boundaries would contain pre-existing cavities as well as being at or near the 45° positions. Furthermore, the pre-existing cavities on boundaries initially at locations away from the 45° positions could have a pinning effect on the boundaries and thus prevent migration to the 45° positions. It is therefore unlikely that pre-existing cavities had any influence on the fatigue behaviour at 350 and 450° C. The main trend demonstrated by the fatigue test results at 450 and 350° C and the lower stress region at 250° C is the increased lives shown by the WQ specimens compared with the FC. The WQ + Age specimens were intermediate in life. Hydride precipitates would be present in the specimens tested at 250° C but not in those tested at 350 and 450° C, but this difference in structure did not influence the order of the fatigue lives. This indicates, therefore, that the hydride precipitate distribution did not have any significant effect during the tests at 250° C and that the differences between the FC and WQ results at 250, 350 and 450° C were associated with residual surface effects from the initial cooling rate from 580° C, such as compressive stresses, twinning and recrystallization in the WQ specimens.

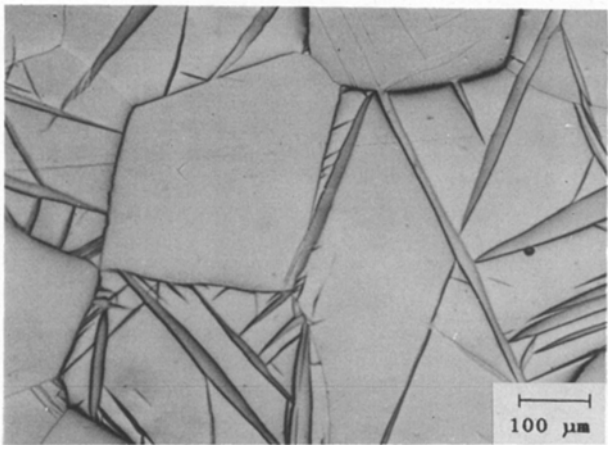

Figure 14 Twinning of surface grains of fatigue test specimens introduced by the WQ treatment.

4.2. Influence of prolonged ageing at 450° C

The effects of ageing at 450° C for 1500 h following a WQ treatment on the fatigue lives at 450° C for samples from batch B are shown in Fig. 21, which also includes the data for samples tested in the FC and WQ as well as some other heat-treated conditions. It is clear that the prolonged ageing had a detrimental effect particularly at low stresses. The degradation in fatigue lives was not due to stresses introduced by the final water quench from 450° C because a furnace cool to room temperature after the prolonged ageing gave the same result. Furthermore, prolonged ageing treatment before the test specimens were machined produced similar reductions in fatigue lives, which suggested that interaction of the specimen surface with the furnace atmosphere at 450° C was not responsible.

To investigate the long-term ageing further, specimens which had received different ageing times were tested at $\pm 3\,\mathrm{MN\,m^{-2}}$, Fig. 22. The fatigue lives decrease gradually with increasing ageing times up

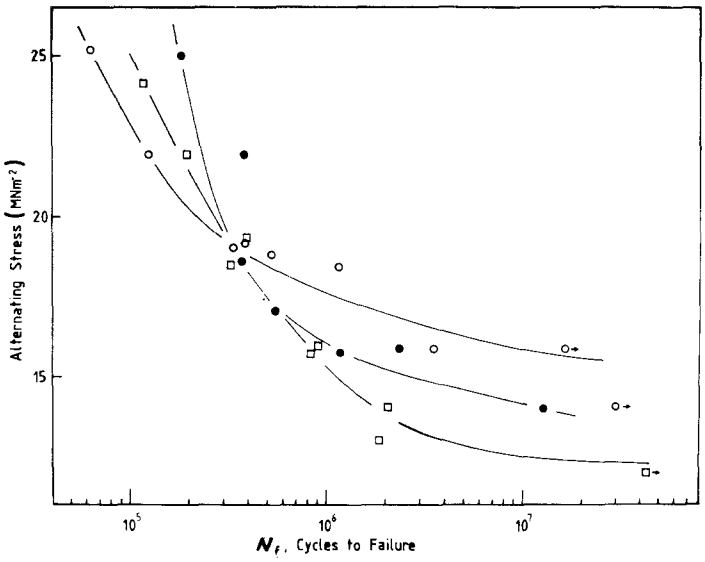

Figure 15 S–N_f curves for fatigue tests at 250° C. (□) FC, (○) WQ, (●) WQ + Age.

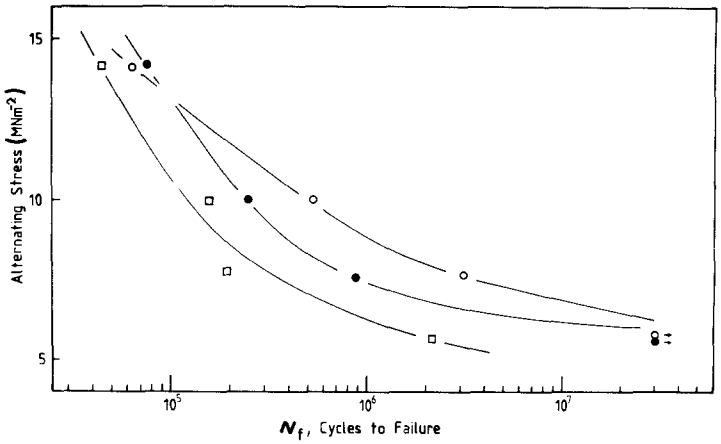

Figure 16 S–N_f curves for fatigue tests at 350° C. (□) FC, (○) WQ, (●) WQ + Age.

to 1500 h when they are comparable to those of the FC specimens. The effect of cooling procedure from 580° C was demonstrated by samples which were slowly cooled from 580 to 350° C, held for 1 h and finally water quenched to RT. Such a treatment might be expected to produce fatigue lives inbetween those of the FC and WQ specimens. The fatigue lives (Fig. 22) were inferior to those of the WQ specimens, but within the scatter band of those of the FC specimens. However, WQ treatment from 580° C after prolonged ageing at 450° C still resulted in a reduced life. This suggests that the deleterious effect of long-term ageing is due to a different cause from that which produces lower fatigue lives in the FC specimens.

Because the failure mode at 450° C is by grain-boundary cavitation, Fig. 20, which is closely associated with grain-boundary sliding [13, 14], grain-boundary orientations (inclinations) with respect to the stress axis would have some influence through the variation of resolved shear stresses with boundary inclination. The boundary-inclination distributions with respect to the stress axis were assessed by analysing the angular distributions of boundary traces on longitudinal sections. Samples tested at $\pm 3\,MN\,m^{-2}$

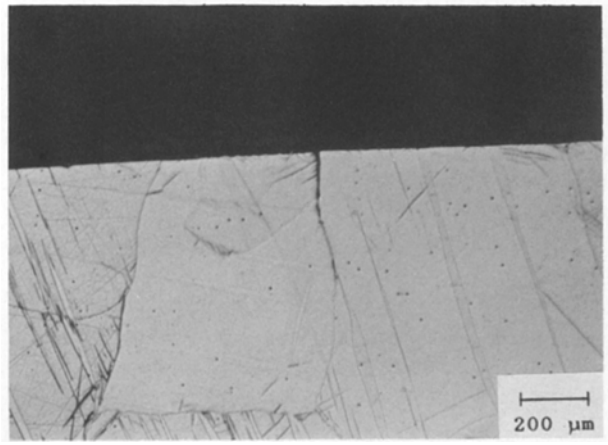

Figure 17 Sectioned surface of an FC specimen after fatigue testing at $\pm 16\,MN\,m^{-2}$ at 250° C.

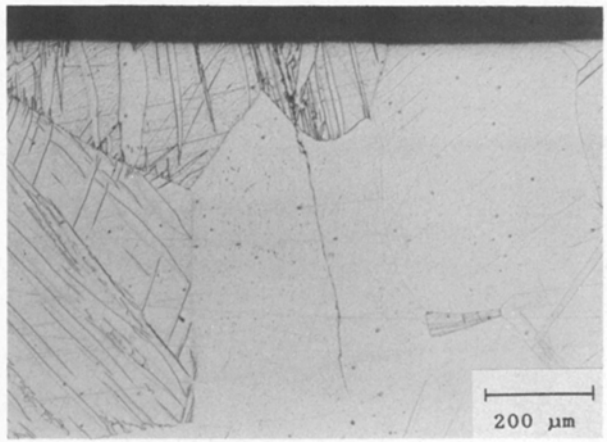

Figure 18 Sectioned surface of a WQ + Age specimen after fatigue testing at $\pm 22\,MN\,m^{-2}$ at 250° C.

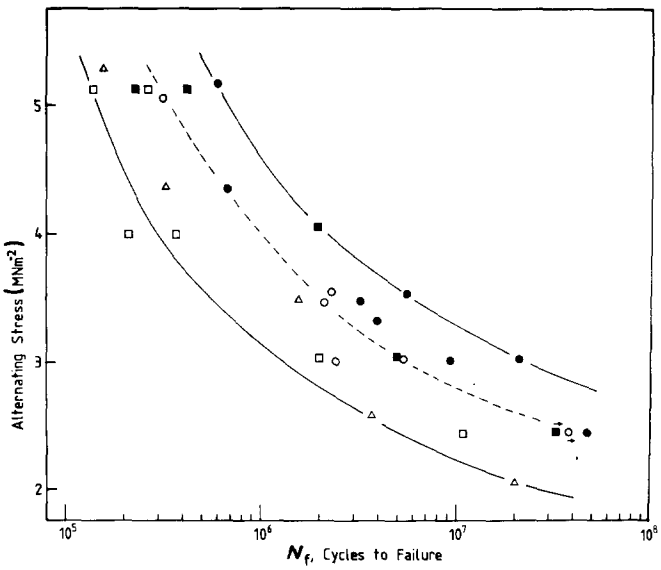

Figure 19 S–N_f curves for fatigue tests at 450° C. (○) Cast A FC, (●) Cast A WQ, (□) Cast B FC, (■) Cast B WQ, (△) Cast C FC.

at 450° C were analysed and the angular distributions for cavitated and non-cavitated boundaries in FC, WQ and 1500 h aged specimens are shown in Figs 23a to f. As expected, the cavitated boundaries, Figs 23a, c and e, are grouped near the 45° positions, while the non-cavitated boundaries, Figs 23b, d and f, complement the distributions for cavitated boundaries and show troughs near the 45° positions. Although these distributions were obtained from sectioned surfaces, the actual angular distributions in three-dimensional space can be derived analytically from the observed boundary trace distributions [21]. This was done for the sample with the 1500 h ageing treatment, Figs 23e and f, and the derived distributions in Fig. 24 show that the observed peak in the range of 30 to 50° C for the cavitated boundaries is accentuated by the transformation. The spurious negative values in some cases are due to the sensitive nature of the transformation, particularly when the observed distributions are subject to statistical fluctuations. Possible changes of the angular distributions during fatigue cycling were analysed by comparing the distribution of boundary traces in the unstressed shoulder sections with that of all boundaries (cavitated and non-cavitated) in the gauge section. The results, in terms of differences in the relative frequencies within each angular range, are shown in Figs 25a, b and c. The FC and WQ specimens show a slightly higher proportion of boundaries at low angles to the stress axis in the gauge sections. For the sample with the long-term ageing, a large proportion of the boundaries in the gauge section are in the angular range of 30 to 60° to the stress axis. Comparison of the boundary trace distributions of the shoulder sections between the WQ specimen and the sample with the long-term ageing showed that the boundary orientations were essentially random in both samples. Assuming that these distributions were representative of the heat-treated but uncycled material, it follows that the peak near 30 to 60° to the stress axis in the gauge section of the aged sample, Fig. 25c, was developed during the fatigue cycling rather than during the 1500 h ageing at 450° C. Furthermore, strain-induced grain-boundary migration took place during the fatigue cycling at 450° C, such that the grain sizes in the gauge sections were typically 0.8 mm compared with 0.5 mm in the shoulder sections. It would thus appear that one effect of the long-term ageing at 450° C was to render the boundaries more prone to cyclic strain-induced migration to positions at 30 to 60° to the stress axis where boundary sliding and cavitation was favoured, thus causing earlier failure.

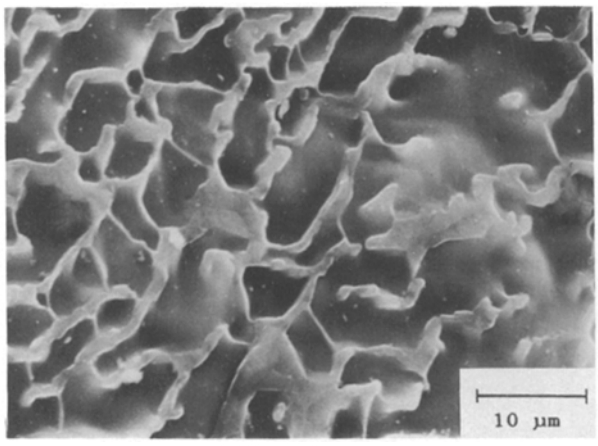

Figure 20 Fracture surface of a WQ specimen after testing at $\pm 3\,MN\,m^{-2}$ at 450° C.

5. Conclusion

The influence of grain-boundary hydride precipitates on the elevated temperature tensile and fatigue properties of Magnox AL80 has been investigated, using three different heat treatments. In addition, the influence of long-term ageing at 450° C on the fatigue lives at that temperature has also been investigated.

At an initial strain rate of 20% h^{-1}, the presence of arrays of grain boundary hydride precipitates in the WQ and WQ + Age specimens at 250 and 300° C resulted in lower ductilities, compared with the FC specimens. This was associated with the formation of intergranular cracks and cavities. At higher temperatures, the WQ + Age specimens showed slightly lower ductilities than the FC and WQ specimens. A possible reason for this was the formation of grain-boundary cavities during the 1 h preheating period

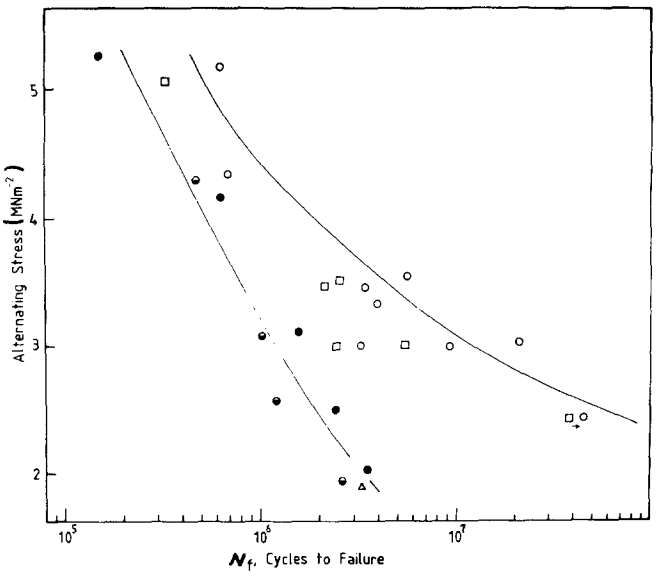

Figure 21 Effects of long term (1500 h) ageing at 450° C on the fatigue lives at 450° C compared with the FC and WQ results in Fig. 19.(□) FC, (○) WQ, (●) WQ + Age at 450° C, (◒) WQ + Age at 450° C before machining specimen, (△) WQ + Age at 450° C with FC to RT.

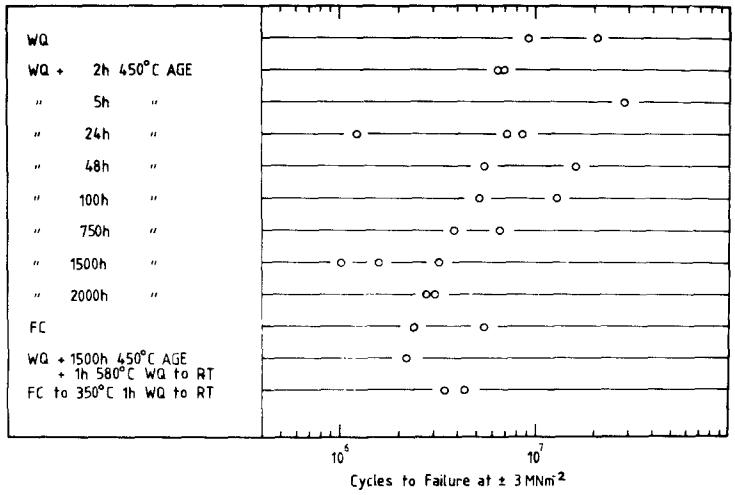

Figure 22 Effects of ageing times at 450° C on the fatigue lives at $\pm 3\,MN\,m^{-2}$ and also the effects of reheat treatment at 580° C. Data also included for the WQ and FC treatment and a treatment involving an initial FC to 350° C followed by WQ.

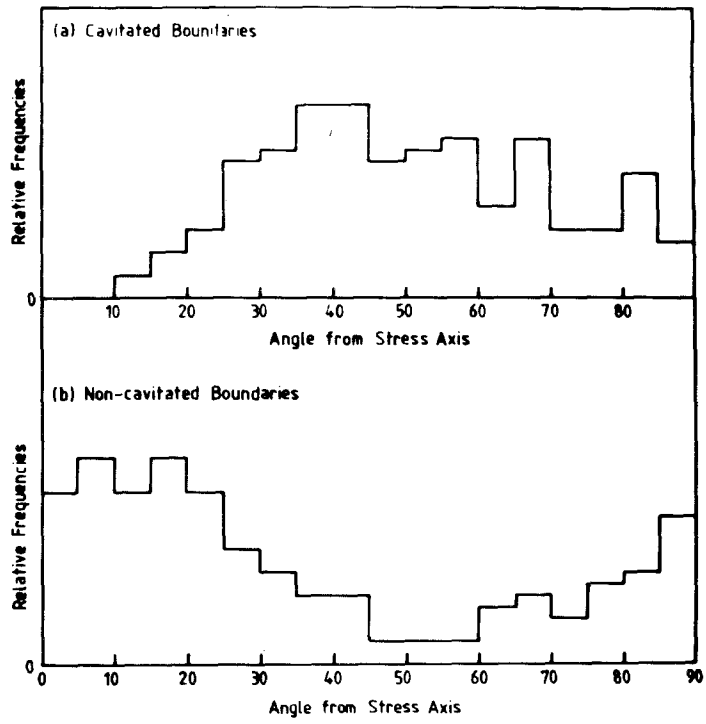

Figure 23 (a) and (b) Angular distribution of the orientation of cavitated and non-cavitated grain-boundary traces with respect to the stress axis in an FC specimen after testing at $\pm 3\,MN\,m^{-2}$ at 450° C. (c) and (d) As for (a) and (b) but for a WQ specimen. (e) and (f) As for (a) and (b) but for the sample with long-term ageing at 450° C.

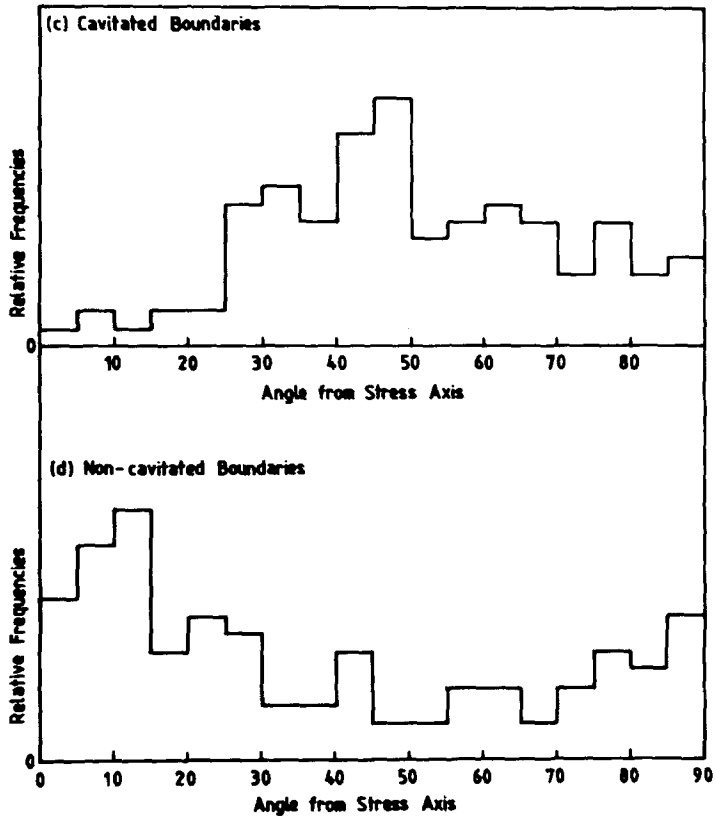

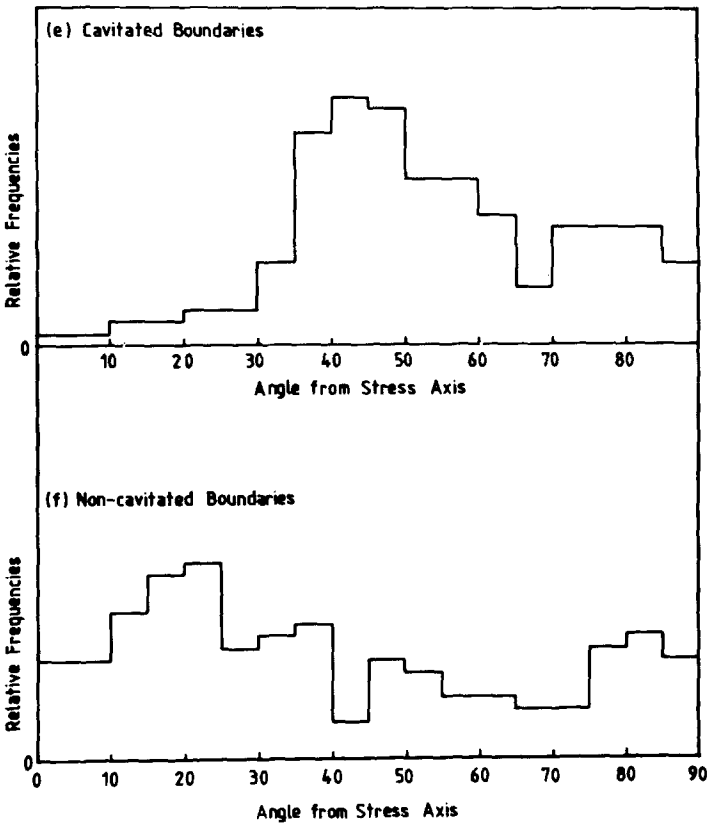

Figure 23 Continued.

prior to testing, caused by the dissociation of the hydride precipitates.

Over the range of strain rates (20 to 2000% h^{-1}) used at 250° C, the lower ductilities of the WQ and WQ + Age specimens as compared with the FC specimens were most evident at the lower rates of strain (20 or 40% h^{-1}).

Following an *in situ* solution treatment at 450° C immediately prior to straining at 20% h^{-1} at 250° C, the ductilities depended on the cooling rate from 450 to 250° C. The effects observed can be interpreted in terms of the changes in the hydride precipitate distribution and also the generation of cavities as a result of hydride dissociation.

The fatigue endurance of Magnox AL80 is not significantly influenced by the grain-boundary hydride precipitates. At room temperature this is due to the mainly transgranular failure mode. At higher tem-

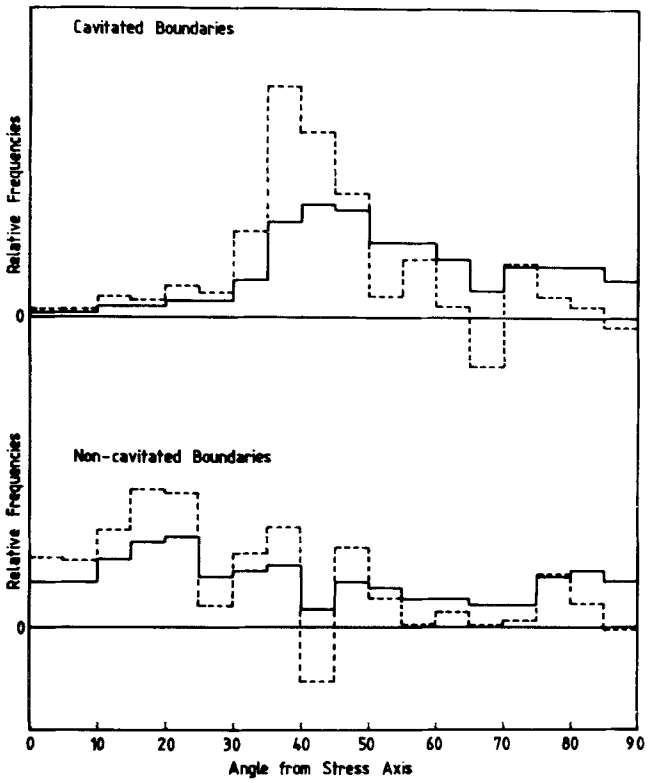

Figure 24 Comparisons of (——) the observed angular distributions of grain-boundary traces (as in Figs 23e and f) with (– – –) the derived distributions.

peratures, where intergranular failures are found it is suggested that the grain boundaries containing the hydride precipitates, or cavities produced by dissociation of the precipitates, were not appropriately orientated to experience high shear stresses. In general, the FC specimens showed lower fatigue lives than the WQ specimens. The longer fatigue endurances of the WQ specimens may have been due to the presence of surface compressive stresses for the lower temperature tests, and the twinning of surface grains produced by the water-quench, leading to the recrystallization of surface grains at higher temperatures.

The fatigue endurance at 450° C of WQ specimens was also reduced by an extended ageing treatment at 450° C prior to testing. This was associated with increased strain-induced migration of grain boundaries during fatigue cycling in a 1500 h aged specimen, although the cause for this is unknown.

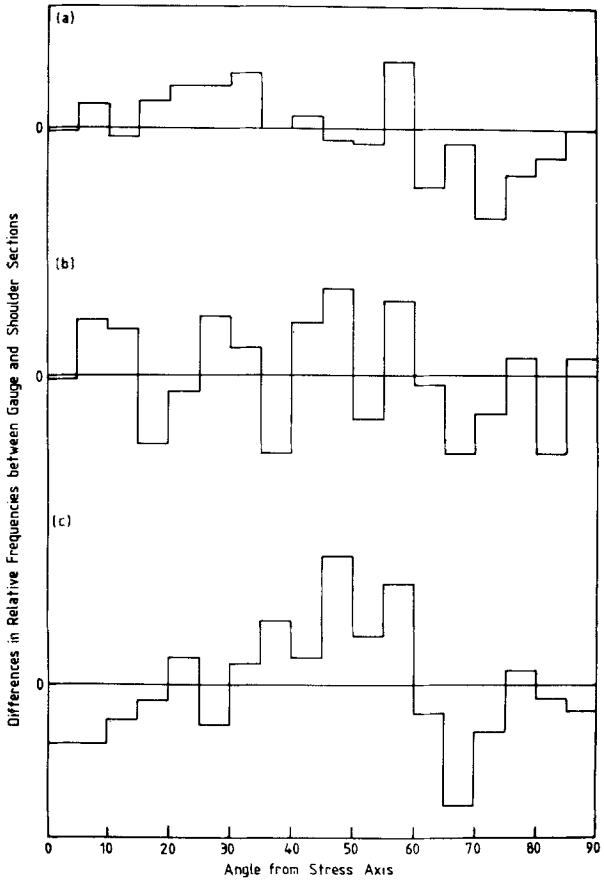

Figure 25 Differences in the relative frequencies of the angular distributions of grain-boundary traces between shoulder sections and gauge sections (cavitated and non-cavitated boundaries) for (a) FC, (b) WQ, and (c) WQ + 450° C Age for 1500 h. Specimens tested at $\pm 3\,MN\,m^{-2}$ at 450° C.

Acknowledgements

The authors thank Professor R. W. K. Honeycombe FRS for the provision of laboratory facilities and the UKAEA Northern Division, Springfields, for a maintenance grant to one of them (YPL) and for the supply of material. They also thank Mr G. A. Burras, Mr E. Ross and Mr R. A. Shaw of UKAEA, Springfields, for many helpful discussions.

References

1. Y. P. LIN and G. C. SMITH, *J. Mater. Sci.* **23** (1988).
2. G. F. HINES, V. J. HADDRELL and R. B. JONES, in "Physical Metallurgy of Reactor Fuel Elements", edited by J. E. Harris and E. C. Sykes (Metals Society, London, 1975).
3. S. S. VAGARALI and T. G. LANGDON, *Acta Metall.* **30** (1982) 1157.
4. P. E. BROOKES, N. KIRBY and W. T. BURKE, *J. Inst. Metals* **88** (1960) 500.
5. P. BOWRING, P. W. DAVIES and B. WILSHIRE, *J. Nucl. Mater.* **22** (1967) 232.
6. A. E. B. PRESLAND and R. I. HUTCHINSON, *J. Inst. Metals* **90** (1962) 239.
7. *Idem, ibid.* **92** (1964) 264.
8. J. E. HARRIS, *Trans. Met. Soc. AIME* **233** (1965) 1509.
9. R. T. RATCLIFFE and G. W. GREENWOOD, *Phil. Mag.* **12** (1965) 59.

10. P. BOWRING, P. W. DAVIES and B. WILSHIRE, *Met. Sci. J.* **2** (1968) 168.
11. H. E. EVANS, *ibid.* **3** (1969) 33.
12. R. DOLDON, *J. Nucl. Mater.* **8** (1963) 169.
13. H. D. WILLIAMS and C. W. CORTI, *Met. Sci. J.* **2** (1968) 28.
14. R. P. SKELTON, *ibid.* **1** (1967) 140.
15. M. V. SPEIGHT and G. W. GREENWOOD, *Phil. Mag.* **9** (1964) 683.
16. D. K. MATLOCK and W. D. NIX, *J. Nucl. Mater.* **56** (1975) 145.
17. S. H. GOODS and W. D. NIX, *Acta Metall.* **26** (1978) 739.
18. R. P. SKELTON, *Phil. Mag.* **14** (1966) 563.
19. J. WEERTMAN, *Met. Trans.* **5** (1974) 1743.
20. R. RAJ and M. F. ASHBY, *ibid.* **2** (1971) 1113.
21. R. A. SCRIVEN and H. D. WILLIAMS, *Trans. Met. Soc. AIME* **233** (1965) 1593.

Received 26 November 1987
and accepted 29 April 1988